Unexpected Materials in a Rembrandt Painting Characterized by High Spatial Resolution Cluster-TOF-SIMS Imaging

ARTICLE *in* ANALYTICAL CHEMISTRY · FEBRUARY 2011

Impact Factor: 5.64 · DOI: 10.1021/ac1017748 · Source: PubMed

6 AUTHORS, INCLUDING:

Jana Sanyova
Royal Institute for Cultural Heritage
31 PUBLICATIONS **191** CITATIONS
SEE PROFILE

Sophie Cersoy
Muséum National d'Histoire Naturelle
8 PUBLICATIONS **33** CITATIONS
SEE PROFILE

Olivier Laprévote
Université René Descartes - Paris 5
245 PUBLICATIONS **4,184** CITATIONS
SEE PROFILE

Alain Brunelle
French National Centre for Scientific Resea…
157 PUBLICATIONS **3,638** CITATIONS
SEE PROFILE

analytical chemistry

ARTICLE

pubs.acs.org/ac

Unexpected Materials in a Rembrandt Painting Characterized by High Spatial Resolution Cluster-TOF-SIMS Imaging

Jana Sanyova,[*,†] Sophie Cersoy,[‡] Pascale Richardin,[*,‡] Olivier Laprévote,[§,⊥] Philippe Walter,[‡] and Alain Brunelle[§]

[†]Institut Royal du Patrimoine Artistique IRPA-KIK, 1 parc du Cinquantenaire, B-1000 Brussels, Belgium

[‡]Laboratoire du Centre de Recherche et de Restauration des Musées de France (LC2RMF), CNRS−UMR 171, Palais du Louvre, Porte des Lions, 14 quai François Mitterrand, 75001 Paris, France

[§]Centre de Recherche de Gif, Institut de Chimie des Substances Naturelles, CNRS, Avenue de la Terrasse, 91198 Gif-sur-Yvette, France

[⊥]Chimie Toxicologie Analytique et Cellulaire, EA 4463, Faculté des Sciences Pharmaceutiques et Biologiques, Université Paris Descartes, 4 avenue de l'Observatoire, 75006 Paris, France

Supporting Information

ABSTRACT: The painting materials of the *Portrait of Nicolaes van Bambeeck* (Royal Museums of Fine Arts of Belgium, Brussels, inv. 155) painted by Rembrandt van Rijn in 1641 has been studied using high resolution cluster-TOF-SIMS imaging. In the first step, a moderate spatial resolution (2 μm) was used to characterize the layer structure and the chemical composition of each layer on account of a high mass resolution. Then, in the second step, and despite a low mass resolution, the cluster primary ion beam was focused well below 1 μm in order to reveal smaller structures in the painting sample. The study confirmed the presence of starch in the second ground layer, which is quite surprising and, at least for Rembrandt paintings, has never been reported before. TOF-SIMS also indicated the presence of proteins, which, added to the size and shape of lake particles, suggests that it was manufactured from shearings (waste of textile manufacturing) of dyed wool, used as the source of the dyestuff. The analyses have also shown various lead carboxylates, being the products of the interaction between lead white and the oil of the binding medium. These findings considerably contribute to the understanding of Rembrandt's studio practice and thus demonstrate the importance and potential of cluster-TOF-SIMS imaging in the characterization on a submicrometer scale of artist painting materials.

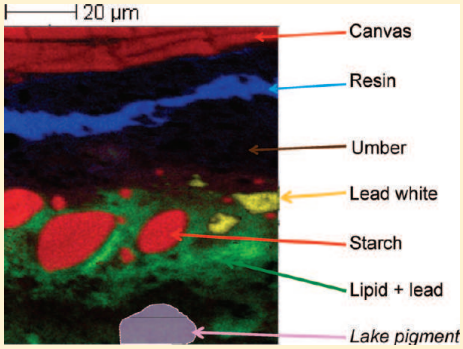

Artist paintings are very complex heterogeneous systems. They are basically superimpositions of several successive layers, each composed of mixtures of various inorganic and organic materials (pigments, extenders, organic binding media, dyestuffs, additives, varnishes, etc.) prepared in the artist studio. The complexity of paint systems is further increased by time-induced transformation and degradation. One approach for a better understanding of such complex paint materials, painting techniques, and studio practices of old masters is to study microsamples, taken from the picture, embedded in a synthetic resin and polished to a flat cross-section. Such cross-sections allow not only the study of the layer structure but also the characterization of the components of each layer. This chemical and physical characterization requires the use of various advanced analytical techniques, including imaging techniques of both mineral and/or organic parts, e.g., scanning electron microscopy with energy dispersive X-ray analysis (SEM-EDX),[1−3] μ-Raman spectroscopy (MRS),[4,5] particle induced X-ray emission (PIXE),[6] X-ray fluorescence (XRF),[7] immunofluorescence microscopy (IFM),[8] Fourier transform infrared microspectroscopy (μFTIR) in various configurations, such as the attenuated total reflection technique (ATR-FTIR) or under synchrotron radiation (SR-FTIR).[9−12]

More recently, time-of-flight secondary ion mass spectrometry (TOF-SIMS) using cluster primary ion beams has become a reference method for surface chemical imaging by mass spectrometry and is particularly relevant in different fields of research on organic or inorganic materials, including cultural heritage studies.[13] Moreover, since the technique explores only the first atomic layers, the damage to the sample is limited and other analytical techniques can be further employed on the same sample to collect some complementary information to correlate with cluster-TOF-SIMS images. With a high sensitivity and selectivity and an excellent lateral resolution (in the order of micrometers), cluster-TOF-SIMS imaging allows the study of painting cross-sections in its integrity. It enables the identification and localization of numerous compounds, either organic or inorganic, that might be present in a painting cross-section without a priori.[14−16]

Received: July 8, 2010
Accepted: December 15, 2010

   dx.doi.org/10.1021/ac1017748 | *Anal. Chem.* XXXX, XXX, 000–000

Figure 1. Portrait of Nicolaes Van Baambeck painted by Rembrandt van Rijn (1641). Royal Museums of Fine Arts (Brussels), inv. 155, © IRPA-KIK, Brussels.

Thus, TOF-SIMS imaging, especially at high spatial resolution, can provide more precise chemical information on the spatial distribution of components in a painting cross-section than elemental analysis techniques (such as SEM-EDX, PIXE, or XRF) or functional group imaging techniques whose spatial resolution are limited to micrometers at the most (such as MRS and μFTIR). On the other hand, cluster-TOF-SIMS imaging requires microsampling and special surface preparation before carrying out analysis, whereas some techniques cited above, such as PIXE and XRF, are absolutely nondestructive (see the comparison of the techniques in Table S1, Supporting Information).

The study of Rembrandt paint materials by TOF-SIMS presented in this paper was carried out on a cross-section of a painting sample from the *Portrait of Nicolaes van Bambeeck* (Royal Museums of Fine Arts of Belgium, Brussels, inv. 155) (Figure 1). Rembrandt van Rijn, one of the most famous Dutch painters of the 17th century, painted in 1641 the portrait of this rich wool merchant.

The *Portrait of Nicolaes van Bambeeck* was restored at the Royal Institute for Cultural Heritage (IRPA-KIK, Brussels, Belgium). During this restoration, the painting technique and the materials of Rembrandt were further studied with many analytical techniques, such as SEM-EDX, MRS, and FTIR on the cross-sections, but also chromatographic methods (GC-MS, HPLC, LC-MS/MS) on scraped fragments.[17] These studies were carried out on six samples taken in 2006 and two older cross-sections prepared during the previous investigation of the Rembrandt ground layers in 1962.[18] Almost all results of these studies were in agreement with numerous earlier studies made on other Rembrandt paintings.[19−22] However, starch, an unexpected component, was revealed in the second greyish layer of the double ground. It was added as an extender to the lead white and was bound with oil. This composition was observed in all microsamples from this painting. It is remarkable that the presence of starch in ground layers of Rembrandt paintings has never been reported before. In this context, it was particularly interesting to take advantage of cluster-TOF-SIMS chemical

dx.doi.org/10.1021/ac1017748 |*Anal. Chem.* XXXX, XXX, 000–000

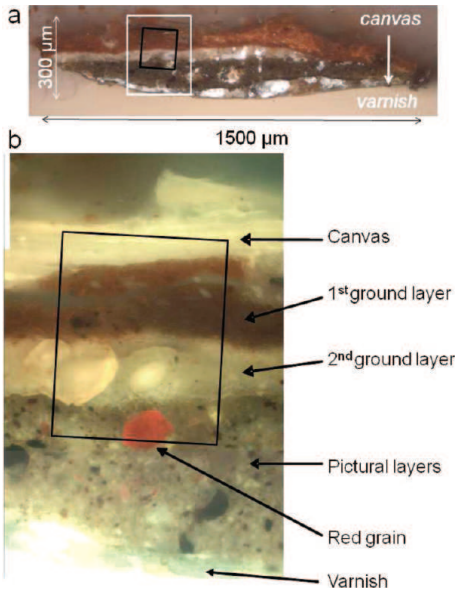

Figure 2. Optical (a) and UV-light microscopic (b) images of the studied painting cross-section. Three layers can be distinguished from the canvas to the varnish: a reddish-orange one, a bright greyish one, and a brown one with a red round-shaped grain. The white rectangle indicates the area investigated by low spatial resolution mass spectrometry imaging whereas the black rectangle indicates the area investigated by high spatial resolution (~80 μm wide).

imaging on one of these samples, since this technique allows the mapping of organic and inorganic materials in a single run, what none of the techniques cited above can do. In the present work, the high resolution cluster-TOF-SIMS images of one of the 1962 cross-sections not only confirmed the presence of starch but also suggested the presence of proteins in the substrate of the red lake and localized the lead soaps in the cross-section.

EXPERIMENTAL SECTION

Sample Surface Preparation. The painting sample had been taken from the dark background of the portrait (Figure 1) and embedded in a resin in 1962. The final resin embedded cross-section was about 1500 μm long, 150 μm high, and 300 μm thick (Figure 2a). To be able to characterize and to localize all the compounds, the flatness of the block surface containing the sample is crucial since cluster-TOF-SIMS is a near-surface analysis technique. It is also important to maintain the embedding block clean, without pollution of any kind. That is the reason why a special but classical procedure of surface flattening, previously described by Mazel et al.,[23] was applied to prepare the cross-section. Briefly, the block is trimmed in order to have the shape of a truncated pyramid and finally cut by ultramicrotomy (0.5 μm) using a Diatome diamond knife (Leica Microsystems, France) until the core of the sample is reached. Trimmed sections could not be used because they did not hold while deposited onto silicon wafers and, in addition, had too many pinholes. Analyses were therefore performed directly on the flat surface of the block itself. To avoid pollution, the block was stored until analysis and carried in a special homemade brass sample holder.

Time-of-Flight Secondary Ion Mass Spectrometry Imaging. Experiments have been performed using a TOF-SIMS IV reflectron-type time-of-flight mass spectrometer (ION-TOF GmbH, Münster, Germany), with a bismuth liquid metal ion gun as the primary ion source. A 25 keV energy Bi_3^+ ion beam was selected with an incidence angle of 45°.[24,25] Secondary ions were extracted with a 2 kV voltage and were postaccelerated to 10 keV kinetic energy just before hitting the detector surface in order to ensure good detection efficiency. A low energy electron flood gun was activated between two successive pulses of the primary ion beam to neutralize any residual charge on the surface of the samples. The settings of the TOF analyzer and of the secondary ion extraction optics are tuned to the kinetic energy of the secondary ions. Their kinetic energy is in fact smaller than 2 keV since they are extracted from the surface of a thick insulating sample, which behaves as a dielectric in the electrostatic extraction field. The procedure, which takes advantage of the capability of the ion reflectron to precisely measure a kinetic energy, is detailed elsewhere.[26]

The ion images have been recorded using successively two different ion source operating modes.[24,25] The so-called `high current bunched mode', which was first used, ensured a moderate 1−2 μm primary ion beam focus and a high mass resolution ($M/\Delta M = 5 \times 10^3$, fwhm at m/z 500) on account of ion pulses of less than 1 ns duration (the pulsed primary ion current was of 0.27 pA for Bi_3^+ ions at a frequency of 10 kHz). Thus, each image was acquired with a lateral resolution of 2 μm and a primary ion dose density (also called `fluence') of 3.3×10^{11} ions·cm^{-2} for each polarity and over a 500 × 500 μm^2 squared area. This first operating mode allowed the precise identification of compounds on account of the high mass resolution and precision. A detailed description of the mass calibration and of the obtained accuracy of a few ppm can be found in a publication of Touboul et al.[27] On the other hand, the `burst alignment mode' provided a higher spatial resolution with a beam focus of ~400 nm but at the expense of the mass resolution (typically unitary) because of a longer pulse duration of about 30 ns. Actually, the longer the pulse, the lower the mass resolution. The pulsed primary ion current was of 0.04 pA for Bi_3^+ ions at a frequency of 10 kHz. Thus, each 100 × 100 μm^2 ion image was acquired with a lateral resolution of 400 nm and a primary ion dose density of 1.8×10^{12} ions·cm^{-2} for each polarity. This second operating mode ensured a precise localization of the compounds. Nevertheless, and although the peaks of interest to generate ionic images must be selected much more carefully than in the `high current bunched mode', images could indeed remain characteristic of one element even with a low mass resolving power. The area investigated was located inside the one analyzed in the first part of the experiments (Figure 2).

The fluence was therefore always maintained below the so-called static SIMS limit[28] and was adjusted according to the scanned area, in order to preserve the molecular information. During the measurement, a TOF mass spectrum was recorded over the area of each pixel. This allows, on the one hand, drawing the spatial distribution of any compound detected at the surface of the sample, and, on the other hand, reconstructing the mass spectrum of any area of the image.

The data acquisition and processing softwares were IonSpec and IonImage (TOF-SIMS 4.1, ION-TOF GmbH, Münster, Germany).

RESULTS AND DISCUSSION

Identification of the Components (high mass resolution). Contour of the Painting Sample in Cross-Section. The contour of the sample embedded in resin was first determined in order

dx.doi.org/10.1021/ac1017748 |*Anal. Chem.* XXXX, XXX, 000–000

to eliminate contributions due to the resin in the mass spectra and also in the ion images. In the positive ion mode, the peak corresponding to the detection of the potassium cation (K^+, m/z 38.96) was selected. Its ion image (Figure S1a, Supporting Information) provided a well-defined and easy to recognize contour of the painting cross-section in resin. In the negative ion mode, an intense ion peak at m/z 85.03 which can be attributed to the $[M - CH_3]^-$ ion of the monomer M of the polymethylmethacrylate (PMMA) resin is also very interesting to delineate the contour of the sample (Figure S1b, Supporting Information). Note that the resin seems to have slightly penetrated into the painting cross-section. Nevertheless, the contours obtained with these ion images in the two different polarities are very similar.

Canvas. Before the painting is created, the canvas must be prepared by application of a ground. Although the grounds generally used by Rembrandt were quite varied, two basic types were often observed, which are the so-called `double ground' and the single quartz ground.[29] The *Portrait of Nicolaes van Bambeeck* is painted on a double-layered ground (Figure 2). The first layer is reddish-orange and applied with a `primer's knife', and the second layer is greyish and was probably rather liquid when spread. This second ground prepares the suitable color and texture of the surface for painting. Next is the gray-brown paint layer, which itself is coated by varnishes which are only visible under UV light illumination (at the bottom of Figure 2b). Note that all the ion images are presented with canvas on the top and varnish at the bottom. The canvas fibers can be observed in the upper part of the UV-microphotographs (Figure 2b). In this area, TOF-SIMS showed the presence of polysaccharide fragment ions (Figure S1c−f, Supporting Information). This could suggest that the canvas of the painting was made of a cellulose-containing material, such as linen, cotton, or hemp. Most probably, it was woven from linen, as usual in Rembrandt canvases.[20] Spectra of cellulose and starch are very similar, and different polysaccharides could not be discriminated only from the spectra. TOF-SIMS also allows visualizing what could be the glue-size on the canvas, on account of the colocalization of various characteristic amino acid fragment ions around and inside the fibers (Figure S1g, Supporting Information): ammonium fragment NH_4^+, m/z 18.04; glycine fragment CH_4N^+, m/z 30.03; alanine fragment $C_2H_6N^+$, m/z 44.05; proline fragment $C_4H_8N^+$, m/z 70.06; valine fragment $C_4H_{10}N^+$, m/z 72.08; lysine fragment $C_5H_{10}N^+$, m/z 84.08; leucine or isoleucine fragment $C_5H_{12}N^+$, m/z 86.10.[23,30]

First Ground Layer. In the first reddish-orange colored ground layer, various metal ions were detected, such as those of magnesium (m/z 23.99), aluminum (m/z 26.98), silicon (Si^+, m/z 27.97 and SiH^+, m/z 28.97), manganese (m/z 54.94), and iron (m/z 55.94). The images of the sum of aluminum- and silicon-containing negative ions are shown in Figure S2a, S2b, and S2c (Supporting Information) and correspond to silicates $(SiO_2)_nOH^-$ (n = 1−3), aluminates $(Al_2O_3)_nOH^-$ (n = 1−2), and $(Al_2O_3)_n(SiO_2)_mOH^-$ (n = 1 with m = 1−2 and n = 2 with m = 2) ions, respectively. A three-color overlay of their respective localizations is shown in Figure S2d (Supporting Information), which suggests that these ions correspond to aluminosilicates,[23] i.e., to a clay earth pigment. The colocalization of iron and manganese ions in this area suggests that umber, which is composed of Fe_2O_3, MnO_2, silica, and Al_2O_3, could have been used. Aluminosilicate ions seem to be also present in smaller amounts in the second ground layer and in the pigment layer. As shown by the dashed lines in Figure S2d (Supporting Information), these first ion images enabled us to draw the different layers of the painting cross-section, which were not as clearly observable from the light microscopic picture (Figure 2a).

Second Ground Layer. In the second greyish ground layer, various lead oxide ions such as $Pb_nO_{n-1}^+$ (n = 1−7), $Pb_nO_{n+1}^+$ (n = 1−7), $Pb_nO_{n-1}OH^+$ (n = 1−5) in the positive ion mode and PbO^-, PbO_2^-, and $(PbO)_n(OH)^-$ (n = 1−6) in the negative ion mode, as well as carbonate ion (CO_3^-, m/z 59.96) were detected. All these ions can be attributed to the presence of lead white,[14] a quite common pigment of which global formula is $2PbCO_3 \cdot Pb(OH)_2$.[31] These assignments were made possible by comparing the mass spectra of a pure reference lead white powder deposited on a silicon wafer (data not shown) with those obtained from the retrospective analysis focused on the specific area where the lead-containing ions were detected in the ion image of Figure 3a. For this comparison, a region of interest (ROI) was selected with the imaging software. The mass spectra extracted in both polarities (Figure S3, Supporting Information) clearly show the peaks characteristic of lead white ions. The optical microscopy shows in the second ground layer the large aggregates, rather pearlescent white particles, which suggest the use of the lead white manufactured by the so-called 'Dutch process' (or stack process).[20]

Another series of peaks was detected in the negative ion mode (m/z 775.82, 777.85, 803.76, 804.77, 805.78, 806.79, 831.80, 832.78, 833.82, 834.82, 859.82, 860.83, 861.84, 862.84, 973.61, and 1001.26), which could be assigned to lead carboxylates (Figure 3b). The corresponding ion image as well as the two-color overlay between lead white and lead carboxylates ions demonstrates that these lead soaps are present not only in the second ground layer but also in the following paint layer (Figure 3c). Indeed, lead may have had interactions with fatty acid carboxylates. Lipid ions are localized in this layer, as can be seen in the image of the sum of fatty acid carboxylates, such as palmitate and stearate, as well as of lower m/z fragment ions (Figure 3d). The colocalization of lead and lipids is not fully surprising, since it is known that lead oxides were often used as additives to the oils in order to make them more siccative.[32] The value of the ratio between palmitate and stearate, calculated from the ratio between the corrected areas of the peaks at m/z 255.24 and 283.28, is 1.35. This indicates that this lipid layer could correspond to linseed oil[33] and is consistent with an assignment to linseed carried out by GC-MS in a previous study (the analysis of the scrapped sample was carried out after the transesterification of fatty acids by MethPrep II during 1 h at 60 °C). This hypothesis is also in agreement with the systematic studies of the Rembrandt painting conducted at the National Gallery (London), which show that linseed oil was the preferred medium of Rembrandt, but also of other artists around him, while walnut oil was sporadically used.[22]

Large size grains of polysaccharide fragment ions in the negative ion mode (CHO_2^-, m/z 45.00; $C_2H_3O_2^-$, m/z 59.01; $C_3H_3O_2^-$, m/z 71.01; $C_4H_5O_3^-$, m/z 99.01) were also detected in this layer.[23] The images of these ions are shown in Figure S1c−f (Supporting Information). The starch is translucent in an oil-binding medium while the lead white is not. This can indicate that the artist could have replaced one part of the lead white by starch or flour used as an extender in order to increase the transparency of this layer.

Paint Brown-Gray Layer. Calcium ions (Ca^+, m/z 39.96; $CaOH^+$, m/z 56.96; $(CaO)_2H^+$, m/z 112.92) were clearly identified and localized in the brown-gray paint layer (Figure 3e−g). These ions were colocalized in the same layer with phosphate

dx.doi.org/10.1021/ac1017748 |*Anal. Chem.* XXXX, XXX, 000–000

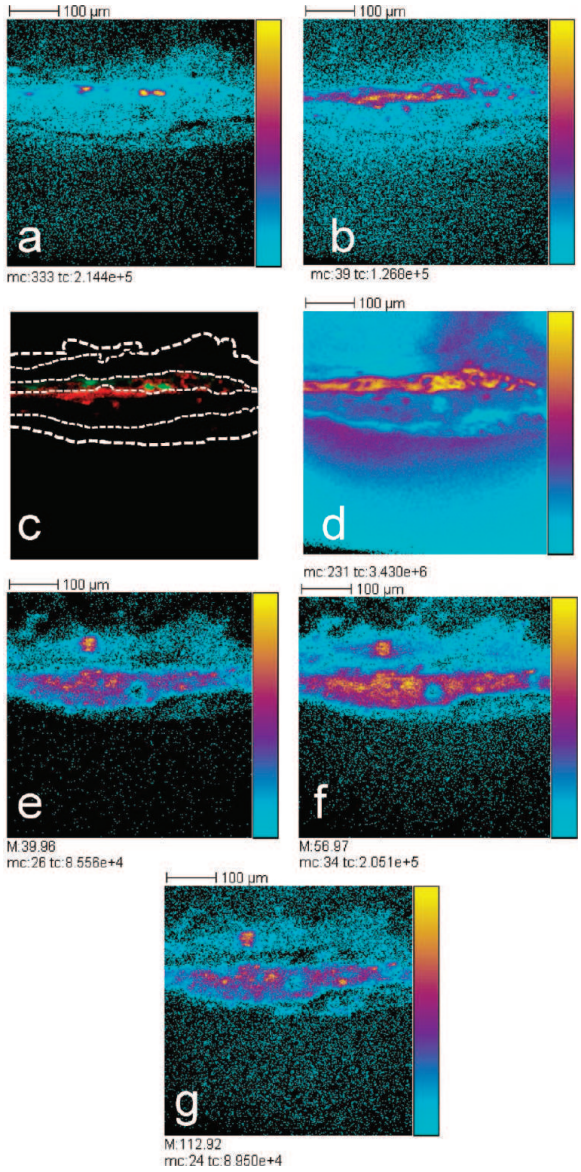

Figure 3. Lead-containing compounds and lipids in the first ground layer: (a) negative ion image of lead white ions (sum of m/z 460.93, 461.93, 462.93, 463.94, and 464.94); (b) negative ion image of lead soap ions (sum of m/z 775.82, 777.85, 803.76, 804.77, 805.78, 806.79, 831.80, 832.78, 833.82, 834.82, 859.82, 860.83, 861.84, 862.84, 973.61, and 1001.26); (c) two-color overlay between lead white ions (green) and lead carboxylate ("soaps") ions (red); (d) negative ion image of fatty acid carboxylates and fragments (m/z 99.05, 113.07, 127.09, 155,12, 169.14, 183.16, 197.18, 211.20, 255.24, 283.28, 284.28, and 211.35). (e−g) Images of calcium hydroxide ions: (e) Ca^+, m/z 39.96; (f) $CaOH^+$, m/z 56.96; (g) $(CaO)_2H^+$, m/z 112.92. Field of view 500 μm × 500 μm; 256 × 256 pixels, pixel size 1.95 μm. Color scale bars, with amplitude in number of counts, are indicated to the right of each ion image. The amplitude of the color scale corresponds to the maximum number of counts mc and could be read as [0, mc]. tc is the total number of counts recorded for the specified m/z (sum of counts in all the pixels).

ions (data not shown). This can indicate the presence of black bones or ivory,[1] which is mostly composed of calcium phosphates such as hydroxyapatite $Ca_5(OH)(PO_4)_3$. The bone black is very often found in the paintings of Rembrandt, frequently mixed with other pigments, such as lake pigments and earth colors.[22] No binder was identified in this layer. Note that these ions containing calcium are also detected in a big grain in the first ground layer.

Varnish. No clear molecular signature from the presence of an old varnish layer could be identified (no pine resin, or no significant amount of lipids on the lower part of the ion images).

Thus, the painting is made of different layers containing both organic and mineral compounds, especially a double ground layer of a white one that is rich in lead white on top of a red one with earth pigment. The mineral part is mostly composed of aluminosilicates, iron, lead, and calcium, whereas the organic part shows the presence of carbohydrates, lipids, and indications for proteins.

High Spatial Resolution. To specify the distribution of the components in the ground layers and to study a red grain visible in the pigmented layer, ion images were acquired with the high spatial resolution mode in order to reach a submicrometer scale. Despite the deterioration of mass resolution, identifications were made possible on account of the above study first driven with high mass resolution. The dramatic difference in mass resolution between the two modes is shown in the spectra of Figure S4 (Supporting Information), which were recorded in the low and high spatial resolutions, respectively, and which show the lead isotopic ions. These ion peaks have then been unambiguously selected to draw the following ion images.

Contours of the Cross-Section. The total ion images recorded in the positive and negative ion modes are shown in Figure 4. Due to a mistake in the settings of the mass spectrometer, the positive and negative ion mode images were slightly shifted in both directions one to each other. It is nevertheless easy to recognize the area which was commonly mapped in the two polarities and which is delimited in Figure 2b and 4. The contours of the different layers could be delimited once more manually.

Embedding Resin. Figure 5a shows a fragment ion (m/z 85) of the PMMA embedding resin, which was found to have penetrated into the sample in the cross-section.

Polysaccharide Fragments. Several fragment ions of polysaccharides chains (CHO_2^-, m/z 45; $C_2H_3O_2^-$, m/z 59; $C_3H_3O_2^-$, m/z 71; $C_4H_5O_3^-$, m/z 99) were again detected and found to be colocalized in the second ground layer. The image of the m/z 59 ion is shown in Figure 5b: carbohydrate grains are clearly visible in the second ground layer and correspond to the circular and ellipsoidal starch particles. Taking into account the size and the shape of the particles, the starch in the second ground may correspond to a wheat starch and was also previously compared to wheat flour grains by μ-Raman spectroscopy (MRS) and identified by liquid chromatography-tandem mass spectrometry (LC-MS/MS). Starch is found in diverse plants, and the size and appearance of its particles is quite characteristic of plants from which they are obtained and so are easily differentiable by optical microscopy after tests with iodine. The starch consists predominantly of two polysaccharides, amylase (smaller particles) and amylopectin (larger particles), which are made of glucose monomers. The starch particles characterized and visualized by TOF-SIMS imaging are composed of `type A' large lenticular-shaped granules (amylopectin, 15−40 $\mu$m, 80−90% in weight, and 20% in number) and of smaller `type B' spherical granules (amylase, 1−10 μm).[34] The relative proportion of type A and type B can influence the structural and functional properties of the wheat starch. It is also known that the granules of wheat starch contain 0.2−0.5% of

dx.doi.org/10.1021/ac1017748 |Anal. Chem. XXXX, XXX, 000–000

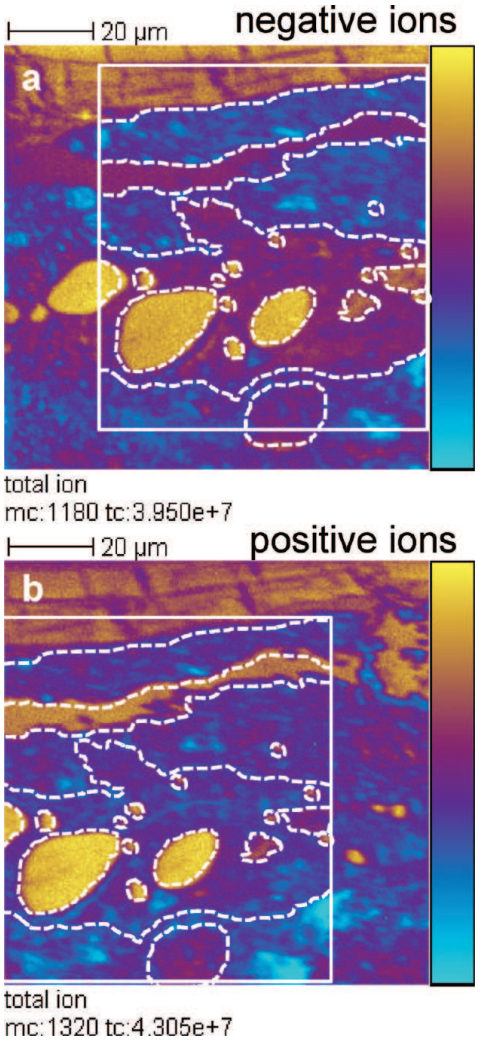

Figure 4. High spatial resolution ion images of the painting cross-section in negative (a) and positive (b) ion modes. Total ion images. Dashed white lines delimit areas of high intensities corresponding to potentially important structures, and white rectangles delimit the common surface between the two images. Field of view 100 μm × 100 μm; 256 × 256 pixels; pixel size 390 nm. Color scale bars, with amplitude in number of counts, are indicated to the right of each ion image. The amplitude of the color scale corresponds to the maximum number of counts mc and could be read as [0, mc]. tc is the total number of counts recorded for the specified m/z (sum of counts in all the pixels).

proteins, 0.5−1.0% of lipids (phospholipids and free fatty acids), and 0.15−0.3% of minerals. This is consistent with Figure 5c, which shows the image of fatty acid carboxylate ions and in which the granules are also visible.

The canvas fibers are also present on the cross-section under the first ground layer (Figure 5b), may correspond to linen cellulose since this textile was widely used in the 17th century canvas paintings, and is also known to be strong and easy to stretch.

Indications for Proteins. Amino acid fragment ions were again detected and colocalized with the cellulosic fiber (Figure 5d), suggesting the presence of glue in the sizing of the canvas. Note that these ions are also detected on the starch grain and in the area of the red grain (visible in Figure 2b) of the brown-gray pigment layer.

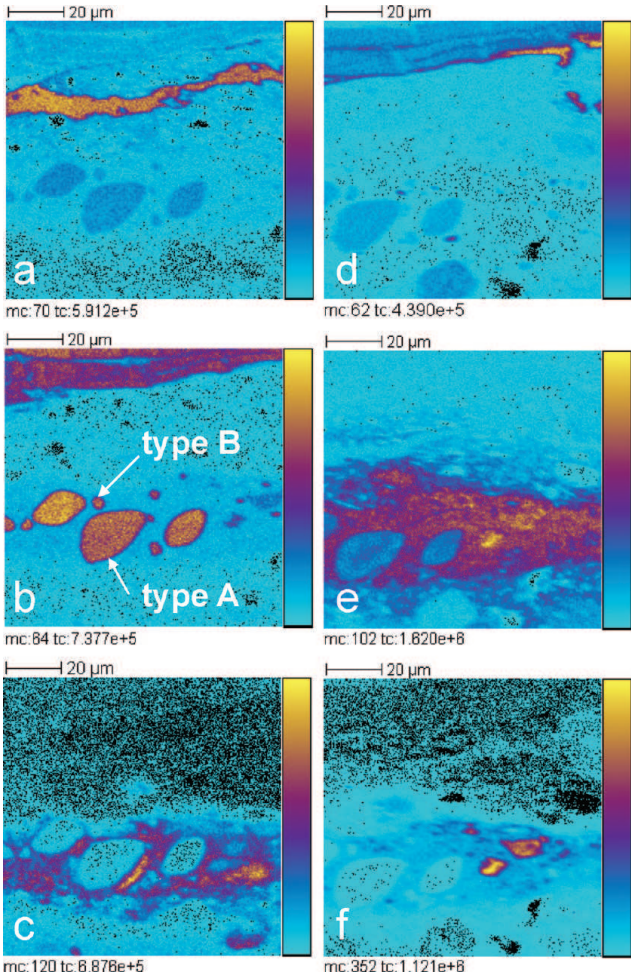

Figure 5. High spatial resolution ion images: (a) ion image of resin fragment ion (m/z 85, probably PMMA), corresponding to the embedding resin, which has gone into the sample cross-section; (b) ion image of a polysaccharide fragment ($C_2H_3O_2^-$, m/z 59), corresponding to wheat starch in the second ground layer and linen on the canvas; (c) ion image of the sum of fatty acid carboxylate ions, corresponding to lipids; (d) ion image of the sum of amino acid fragment ions, corresponding to proteins on the canvas; (e) ion image corresponding to the sum of lead positive ions (Pb^+, Pb_2^+, and Pb_3^+). (f) Sum of ion images corresponding to lead white. Field of view 100 μm × 100 μm; 256 × 256 pixels; pixel size 390 nm. Color scale bars, with amplitude in number of counts, are indicated to the right of each ion image. The amplitude of the color scale corresponds to the maximum number of counts mc and could be read as [0, mc]. tc is the total number of counts recorded for the specified m/z (sum of counts in all the pixels).

Lipids and Lead. While the image corresponding to the sum of the palmitate and stearate ions (m/z 255 and 283) is shown in Figure 5c, the image of the sum of lead and lead cluster ions (Pb_n^+, n = 1−3) is shown in Figure 5e. The colocalization between lipids and lead compounds in this layer is confirmed. The image corresponding to the sum of lead white ions is shown in Figure 5f. Starch grains are found to be located very close to the lead white, in the second ground layer.

Substrate of Red Lake. Figure S5a and S5b (Supporting Information) shows that the localization of aluminum ions (Al^+, m/z 27) and of amino acid fragment ions (ammonium NH_4^+, m/z 18; glycine fragment CH_4N^+, m/z 30; alanine fragment

dx.doi.org/10.1021/ac1017748 |Anal. Chem. XXXX, XXX, 000–000

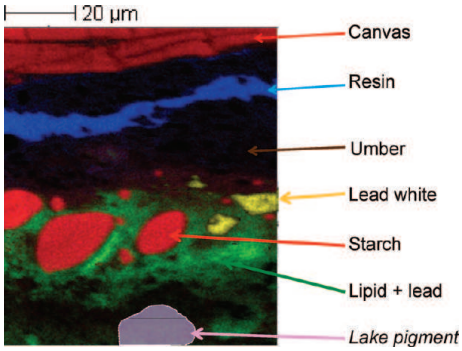

Figure 6. Summary of the chemical composition and localization obtained with an overlay of most of the TOF-SIMS results and showing the stratigraphy of the painting cross-section. Scale bar 20 μm.

$C_2H_6N^+$, m/z 44; proline fragment $C_4H_8N^+$, m/z 70; valine fragment $C_4H_{10}N^+$, m/z 72; lysine fragment $C_5H_{10}N^+$, m/z 84; leucine or isoleucine fragment $C_5H_{12}N^+$, m/z 86) coincide with the large particle of red lake visible in the paint layer on the Figure 2b.

The lake is a pigment composed of the cation−organic dyestuff complex or salt and of a substrate, on which the complex is fixed by adsorption or chemisorption. The red dyestuffs at the time of Rembrandt were extracted from natural compounds, the most frequently used being madder plants (*Rubia tinctorum* L.), Mexican cochineal (*Dactylopius coccus* Costa), or Bresil wood (*Caesalpinia* sp.). The most frequent cation was aluminum, but calcium could also be found in the lake pigments. The physical and chemical properties of the lakes depend on the dyestuff and of the cation, as well as on the manufacturing process.[35] Indications of the presence of proteins in the red lake used by Rembrandt indicate that, as suggested by the study of historical written sources,[36] it was prepared from shearings of dyed cloth, the waste from textile industry, rather than directly from raw materials. Also note that the particles of the lake do not contain calcium, as usually observed in lake pigments.

Synthesis. The *Portrait of Nicolaes van Bambeeck* is painted on a gray-on-red double ground. The first ground contains red-brown earth pigments. The second ground, light gray and linseed oil-based, contains lead white and large and small oval particles of starch. Above these ground layers, the oil paint layer is composed mainly of calcium carbonate, aluminosilicates, and large particles of black bone pigment, and the red lake which is composed of aluminum- and protein-containing substrates. Some lead carboxylates are localized in this paint layer on the border with the second ground layer. Animal glue was likely used for the sizing of the canvas.

An overlay of most of the ion images obtained by TOF-SIMS is shown in Figure 6 to visually sum the spatial distribution of the chemical compounds displayed in the painting cross-section by the high spatial resolution analysis: canvas in linen cellulose, PMMA embedding resin that has gone into the first ground layer and umber, lipids with lead white and wheat starch grains in the second ground layer, and red lake pigment grains in the pigment layer.

CONCLUSION

High resolution cluster-TOF-SIMS imaging has proved to be a very interesting tool to characterize the nature and to map the distribution of various organic and mineral chemical compounds in a complex, multilayered painting cross-section, in one single experiment. High spatial resolution was very important and useful to get a precise imaging of various compounds of each layer in the paint system of the *Portrait of Nicolaes van Bambeeck*, such as mineral and organic pigments, binding media, additives, and degradation products. In addition, the glue-sizing of the cellulosic canvas was also illustrated. Overlays of images from different single ion species enabled us to consider possible unexpected interactions between neighboring components. This is exemplified by lipids from the binder with lead white, which seem to have given a potentially dangerous growth of lead carboxylates or maybe lead soaps, which could thus involve future degradations of the painting.[37] The characterization as well as the distribution of compounds in the multilayered paint system of Rembrandt by TOF-SIMS on a submicrometer scale improves the understanding of Rembrandt studio practice of this 17th century master, who is known as a very ingenious and inventive artist−experimentalist.

Such TOF-SIMS layered analysis could, in the future, be achieved on other kinds of complex biological or archeological samples made of hybrid materials (i.e., containing both mineral and organic compounds) and may help to understand their supramolecular spatial organization and evolution without putting their integrity at risk.

ASSOCIATED CONTENT

Supporting Information. Additional information as noted in the text. This material is available free of charge via the Internet at http://pubs.acs.org.

AUTHOR INFORMATION

Corresponding Author

*E-mail: jana.sanyova@kikirpa.be; pascale.richardin@culture.gouv.fr.

ACKNOWLEDGMENT

The authors thank all collaborators of IRPA-KIK who participated in the study of the *van Bambeeck* painting technique by Rembrandt: Cécile Glaude, Françoise Rosier, Hélène Dubois, Steven Saverwyns, Wim Fremout, and Géraldine Van Ovenstraeten. The authors are also very grateful to Danielle Jaillard from the Centre Commun de Microscopie Électronique (UMR CNRS 8080, Orsay, France) for ultramicrotomy preparation. This study of a cross-section by TOF-SIMS was carried out in the frame of NACHO Inter-University Attraction Pole P6/16 financed by the Belgian Science Policy.

REFERENCES

(1) Adrians, A.; Dowset, M. G. In *Non-destructive Microanalysis of Cultural Heritage Materials*; Janssens, K.; Van Grieken, R., Eds.; Elsevier Science B.V.: New York, 2004; pp 73−128.

(2) Loon, A.; Boon, J. J. *Spectrochim. Acta B* **2004**, *59*, 1601–1609.

(3) Lau, D.; Villis, C.; Furman, S.; Livett, M. *Anal. Chim. Acta* **2008**, *610*, 15–24.

(4) Nevin, A.; Loring Melia, J.; Osticioli, I.; Gautier, G.; Colombini, M. P. *J. Cult. Herit.* **2008**, *9*, 154–161.

(5) Fremout, W.; Saverwyns, S.; Peters, F.; Deneffe, D. *J. Raman Spectrosc.* **2006**, *37*, 1035–1045.

(6) de Viguerie, L.; Beck, L.; Salomon, J.; Pichon, L.; Walter, P. *Anal. Chem.* **2009**, *81*, 7960–7966.

(7) Herrer, L. K.; Montalbani, S.; Chiavari, G.; Cotte, M.; Solé, V. A.; Buenoe, J.; Duran, A.; Justo, A.; Perez-Rodriguez, J. L. *Talanta* **2009**, *80*, 71–83.

(8) Vagnini, M.; Pitzurra, L.; Cartechini, L.; Miliani, C.; Brunetti, B. G.; Sgamelotti, A. *Anal. Bioanal. Chem.* **2008**, *392*, 57–64.
(9) Joseph, E.; Prati, S.; Sciutto, G.; Ioele, M.; Santoprade, P.; Mazzeo, R. *Anal. Bioanal. Chem.* **2010**, *396*, 899–910.
(10) Mazzeo, R.; Joseph, E.; Prati, S.; Millemaggi, A. *Anal. Chim. Acta* **2007**, *599*, 107–117.
(11) Spring, M.; Ricci, C.; Peggie, D.; Kazarian, S. G. *Anal. Bioanal. Chem.* **2008**, *392*, 37–45.
(12) Cotte, M.; Dumas, P.; Taniguchi, Y.; Checroun, E.; Walter, P.; Susini, J. *C.R. Phys.* **2009**, *10*, 590–600.
(13) Mazel, V.; Richardin, P. In *Organic Mass Spectrometry in Art and Archaeology*; Colombini, M. P.; Modugno, F., Eds.; Wiley: New York, 2009; pp 433−457.
(14) Keune, K.; Boon, J. J. *Anal. Chem.* **2004**, *76*, 1374–1385.
(15) Keune, K.; Hoogland, F.; Boon, J. J.; Peggie, D.; Higgitt, C. *Int. J. Mass Spectrom.* **2009**, *284*, 22–34.
(16) Boon, J. J.; Keune, K.; van der Weerd, J.; Geldof, M.; van Asperen de Boer, J. R. J. *Chimia* **2001**, *55*, 952–960.
(17) Sanyova, J.; Saverwyns, S.; Fremout, W. A surprising ground layer in Rembrandt's Portrait of Nicolaes van Bambeeck. Poster presentation at The National Gallery Technical Bulletin 30th Anniversary Conference: Studying Old Master Paintings - Technology and Practice, Sept 16−18, 2009, London, and Proceedings of the National Gallery Technical Bulletin 30th Anniversary Conference, Archetype Publications, London, in press.
(18) Coremans, P.; Thissen, J. *Bull. R. Inst. Cult. Herit. IRPA-KIK* **1964**, *7*, 187–95.
(19) Broos, B.; Wadum, J. In *Rembrandt under the Scalpel*; Middelkoop, N. N.; Noble, P.; Wadum, J.; Broos, B., Eds.; Mauritshuis: The Hague, The Netherlands, 1998; pp 47−72.
(20) Roy, A.; Bomford, D.; Kirby, J.; White, R. In *Art in the making. Rembrandt*, Eds: Bomford, D.; Kirby, J.; Roy, A.; Rüger, A., White, R. National Gallery: London, 2006, pp 27−51.
(21) Groen, K. M. In *A corpus of Rembrandt paintings IV: the Self-Portraits*; Van de Wetering, E., Ed.; Springer: New York, 2005; pp 318−334.
(22) White, R.; Kirby, J. *Natl. Gallery Tech. Bull.* **1994**, *15*, 64–78.
(23) Mazel, V.; Richardin, P.; Touboul, D.; Brunelle, A.; Walter, P.; Laprévote, O. *Anal. Chim. Acta* **2006**, *570*, 34–40.
(24) Sodhi, R. N. S. *Analyst* **2004**, *129*, 483–487.
(25) Brunelle, A.; Touboul, D.; Laprévote, O. *J. Mass Spectrom.* **2005**, *40*, 985–999.
(26) Seyer, A.; Einhorn, J.; Brunelle, A.; Laprévote, O. *Anal. Chem.* **2010**, *82*, 2326–2333.
(27) Touboul, D.; Brunelle, A.; Halgand, F.; De La Porte, S.; Laprévote, O. *J. Lipid Res.* **2005**, *46*, 1388–1395.
(28) Vickerman, J. C. TOF-SIMS - an overview. In *ToF-SIMS - Surface Analysis by Mass Spectrometry*; Vickerman, J. C., Briggs, D., Eds.; Surface Spectra and IM Publications: Manchester and Chichester, U.K., 2001; pp 1−40.
(29) Groen, K. M. *Art Matters − Netherlands Tech. Stud. Art* **2005**, *3*, 138–154.
(30) Sanni, O. D.; Wagner, M. S.; Briggs, D.; Castner, D. G.; Vickerman, J. C. *Surf. Interface Anal.* **2002**, *33*, 715–728.
(31) Welcomme, E.; Walter, P.; Bleuet, P.; Hodeau, J. L.; Dooryhee, E.; Martinetto, P.; Menu, M. *Appl. Phys. A: Mater. Sci. Process.* **2007**, *89*, 825–832.
(32) Cotte, M.; Checroun, E.; Susini, J.; Walter, P. *Appl. Phys. A: Mater. Sci. Process.* **2007**, *89*, 841–848.
(33) Mills, W.; White, R. *The Organic Chemistry of Museum Objects*, 2nd ed.; Butterworth-Heinemann: Boston, 2003.
(34) Salman, H.; Blazek, J.; Lopez-Rubio, A.; Gilbert, E. P.; Hanley, T.; Copeland, L. *Carbohyd. Polym.* **2009**, *75*, 420–427.
(35) Sanyova, J. *Proceedings of congrès Art et chimie. La couleur*, Paris, Sept 16−18, 1998, Goupy, J.; Mohen, J.-P., Eds.; CNRS Editions, Paris, 2000, pp 14−17.
(36) Kirby, J.; Spring, M.; Higgitt, C. *Natl. Gallery Tech. Bull.* **2005**, *26*, 71–87.
(37) Plater, M. J.; De Silva, B.; Gelbrich, T.; Hursthouse, M. B.; Higgitt, C. L.; Saunders, D. R. *Polyhedron* **2003**, *22*, 3171–3179.